DOI: 10.1002/cssc.201200305

STEP Wastewater Treatment: A Solar Thermal Electrochemical Process for Pollutant Oxidation

Baohui Wang,*[a, b] Hongjun Wu,[a] Guoxue Zhang,[a] and Stuart Licht*[b]

A solar thermal electrochemical production (STEP) pathway was established to utilize solar energy to drive useful chemical processes. In this paper, we use experimental chemistry for efficient STEP wastewater treatment, and suggest a theory based on the decreasing stability of organic pollutants (hydrocarbon oxidation potentials) with increasing temperature. Exemplified by the solar thermal electrochemical oxidation of phenol, the fundamental model and experimental system components of this process outline a general method for the oxidation of environmentally stable organic pollutants into carbon dioxide, which is easily removed. Using thermodynamic calculations we show a sharply decreasing phenol oxidation potential with increasing temperature. The experimental results demonstrate that this increased temperature can be supplied by solar thermal heating. In combination this drives electrochemical phenol removal with enhanced oxidation efficiency through (i) a thermodynamically driven decrease in the energy needed to fuel the process and (ii) improved kinetics to sustain high rates of phenol oxidation at low electrochemical overpotential. The STEP wastewater treatment process is synergistic in that it is performed with higher efficiency than either electrochemical or photovoltaic conversion process acting alone. STEP is a green, efficient, safe, and sustainable process for organic wastewater treatment driven solely by solar energy.

Introduction

In recent years, there has been increasing interest in finding innovative solutions for the efficient removal of organic pollutants from wastewater.[1–2] Generally, wastewater treatment is conducted using primary, secondary, or tertiary methods (which includes removal or neutralization of macroscopic, chemical, or biological contaminants from water), depending on the nature of the pollutants. The character of several organic pollutants renders biodegradation treatment ineffective. For this reason, physicochemical methods, typically oxidation by chlorine or ozone, are used. However these methods have disadvantages which include high energy consumption (usually from fossil fuels) for the preparation and distribution of these oxidants, and in the case of chlorine-containing oxidants, safe storage and the possible formation of unhealthy chloro-carbon intermediates are also challenges.[3] An alternative can be the application of electrochemical technologies for wastewater treatment, which bring the advantages of versatility, environmental compatibility, and potential effectiveness.[4–7] Both direct and mediated electrochemical oxidations can be considered, which bring new opportunities to research and industries seeking new technologies for wastewater treatment. Briefly, electrochemical treatment is performed by direct (negative and/or positive charge) and/or indirect (oxidant and/or reductant) action, similar to chemical decomposition. The electrolysis of dissolved organic pollutants has been previously investigated at or near room temperature in aqueous media, where the endothermic processes are constrained by high electrolysis rest potentials, large overpotentials, low electrolysis rates, and low electrolysis efficiencies. Organic pollutants that are difficult to degrade can exhibit a complex reactivity, but can often be electrochemically oxidized at an anode. However, the energy cost of such processes is typically high (a large electrolysis voltage is required), yields are low, and ultimately only a small fraction of the organic component is removed.[1,2]

Solar energy is considered a green fuel for the 21st century, with much of the attention focused on the solar generation of electricity or fuel.[8] Solar thermal electrochemical production (STEP) is a process that is fundamentally different from photovoltaic or photoelectrochemical solar energy conversion processes, utilizing the complete solar spectrum to decrease the energy required to drive useful electrochemical processes including metals production and carbon capture.[8–16] Here, the STEP process brings an alternative approach to the development of organic wastewater treatment providing a clean, renewable, and cost effective methodology. We use as an example, the effective treatment and removal of phenol an especially harmful organic pollutant in wastewater.[17] Conventional chlorination treatment of phenol generates undesired chlorophenol byproducts.[17] The importance of phenol wastewater treatment and the challenges of alternative electrochemical and photo-electrocatalytic approaches have been of intense interest in the recent literature.[17–38]

[a] Prof. B. Wang, Prof. H. Wu, G. Zhang
Institute of New Energy Chemistry and Environmental Science
College of Chemistry and Chemical Engineering
Northeast Petroleum University
Daqing 163318 (PR China)
E-mail: wangbh@nepu.edu.cn

[b] Prof. B. Wang, Prof. S. Licht
Department of Chemistry
George Washington University
Washington, DC 20052 (USA)
E-mail: slicht@gwu.edu

One renewable path towards organic pollutant oxidation is to utilize energy from the visible region of the solar spectrum to produce electricity for electro-oxidation. Another path is to utilize solar heat to directly oxidize organic pollutants by thermochemistry. The thermal oxidation of organic pollutants requires excessive temperatures, while the electro-oxidation is ineffective due to high overpotentials and low current densities at room temperature. However, these processes can be combined to result in a lower-temperature process, which can be carried out at elevated, but not excessive, temperatures (compatible with the constraints of high-temperature materials) by using coupled electrochemical reactions with high system efficiency.

STEP originates from our theory for the use of solar thermal energy to decrease the energy needed to drive endothermic electrolysis processes.[9] Experimental support for our STEP theory includes water splitting for hydrogen production;[8,15] removal of atmospheric and smokestack carbon dioxide by the electrochemical degradation into carbon and oxygen;[11] and useful chemical syntheses, including iron metal from iron ore (hematite), as well as Cl_2, Mg, and Na from the chloride salts found in seawater;[10,12,13] fuels,[14,15] and calcium oxide.[16] In this paper, we extend STEP theory and experiments to solar driven efficient wastewater treatment. The STEP chemistry of wastewater treatment involves (i) the absorption of solar thermal energy to reduce the energy required to oxidize pollutants, (ii) the conversion of energy from the visible region of the solar spectrum to generate electric charge for electrolysis, and (iii) the low-energy electrolysis of pollutants, here exemplified by STEP oxidation of phenol. A theory of STEP wastewater treatment is provided and thermodynamic calculations support the experimental demonstration of the STEP wastewater treatment process. As with our previous studies, we use the convention of $E_{electrolysis} = \Delta G/nF$ to describe the positive potential necessary to drive a nonspontaneous electrolytic reduction.[9,10] Experimentally, it is demonstrated that at elevated temperatures, the organic pollutants are activated by decreasing their oxidation potential and improving their kinetics, to facilitate effective electrolytic oxidation to CO_2. This opens a pathway to thermo-electrochemical oxidation at a greater efficiency than either electrochemical or the photovoltaic (PV) driven processes alone.

Results and Discussion

Basic STEP theory

As shown in Scheme 1 A, a single, small-band-gap semiconductor junction, such as in a silicon photovoltaic cell, cannot generate the minimum photopotential required to drive many room temperature electrolysis reactions, such as water electrolysis to generate hydrogen. In the past, research to facilitate this process has focused on tuning the semiconductor band gap, E_g, to provide a better match to the electrochemical potential,[39] or by utilizing multiple photon excitation via more complex, multiple-band-gap structures.[40,41] Neither single- nor multiple-band-gap structures are capable of excitation beyond the band edge and therefore neither make use of longer wavelength sunlight. Hence, photovoltaics are limited to super-band-gap sunlight, $h\nu > E_g$, and sub-bandgap, long-wavelength, solar thermal radiation is wasted by these devices.

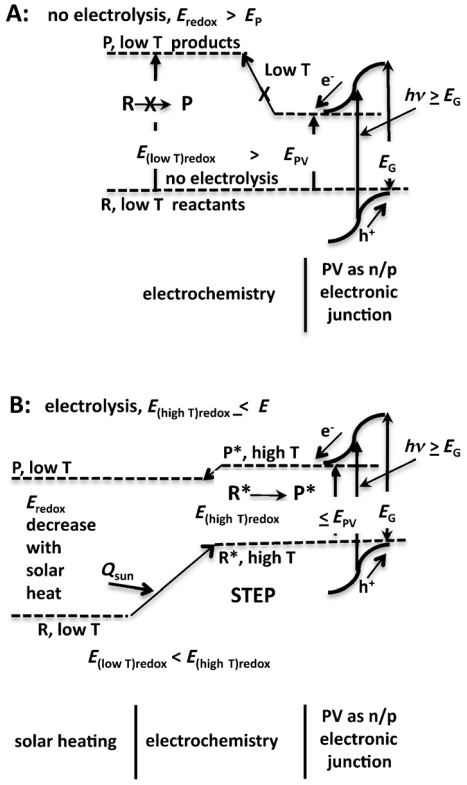

Scheme 1. Comparison of PV and STEP solar driven electrolysis energy diagrams. The STEP process uses sunlight to drive otherwise energetically-forbidden pathways of charge transfer. The energy of photodriven charge transfer is insufficient (A) to drive (unheated) electrolysis, but is sufficient (B) to drive endothermic electrolysis in the solar heated STEP. The STEP process uses both visible and thermal solar energy for higher efficiency; the thermal decreases the electrolysis potential forming an energetically-allowed pathway to drive electrochemical charge transfer.

The STEP process directs IR sunlight, which is not capable of driving photovoltaic charge separation, to heat endothermic electrochemical reaction mixtures, while retaining use of the visible sunlight at shorter wavelengths to generate electric charge for driving the electrolysis. Hence, rather than tuning the band gap to provide a better energetic match to the electrolysis potential, the STEP process instead tunes the redox potential to match the band gap.[15,42]

Scheme 1 B presents the energy diagram of a STEP process. The high temperature pathway enabled by STEP decreases the free energy requirements for processes in which the electrolysis potential decreases with increasing temperature. In the STEP process the solar energy is used to drive pathways of charge transfer, which are otherwise energetically forbidden. As illustrated at the top of Scheme 2, by using STEP we can utilize radiation that is of sufficient energy to drive PV charge transfer, and then apply sub-band-gap and excess super-band-gap radiation to increase the temperature within the electrolysis chamber. The light harvesting can be carried out in various optical configurations; for example, in lieu of parabolic, or Fres-

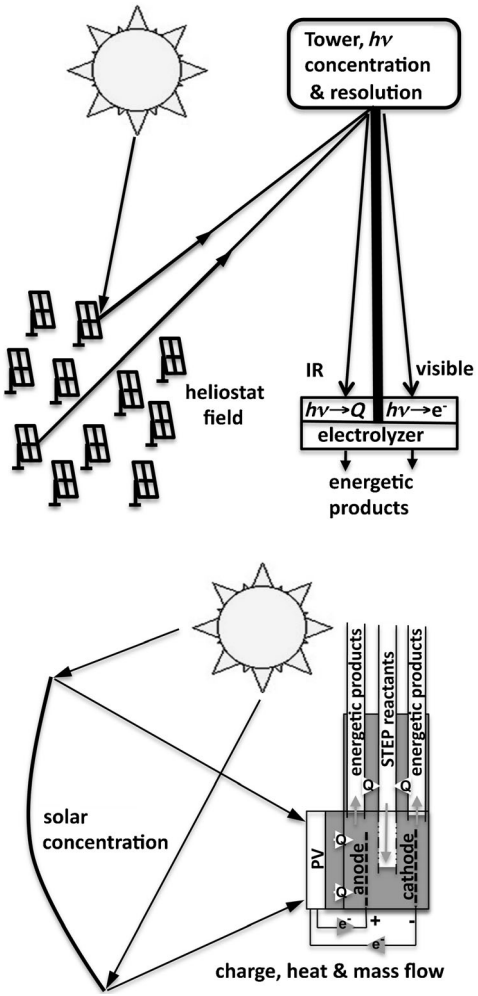

Scheme 2. Global use of sunlight to drive the formation of energy-rich molecules. Top: Beam splitters redirect sub-band-gap sunlight away from the PV onto the electrolyzer.[11,15] Light harvesting can use various concentrators in the STEP process.[9] Bottom: Charge, & heat flow in STEP, showing heat flow, electron flow, and reagent flow.

nel, concentrators, a heliostat/solar tower can be used. STEP is intrinsically more efficient than other solar energy conversion processes,[11,14] as it synergistically utilizes not only the visible sunlight used to drive PVs, but also utilizes the previously detrimental (due to photovoltaic thermal degradation) thermal component of sunlight, for the electrolysis.

The lower portion of Scheme 2 summarizes the charge, heat, and molecular flows for the STEP treatment. As illustrated in the scheme, heat is recovered from the products for use in heating the incoming reactants. In this specific case, with the STEP process for phenol oxidation, the outgoing, heated water can be used to heat the incoming wastewater, and the hydrogen generated as a treatment byproduct is a useful fuel. The high-temperature pathway decreases the potential required to drive the endothermic electrolysis process, and it also improves the kinetics of charge transfer (i.e., decreases overpotential losses), which governs the electrolysis. The extent of the decrease in the electrolysis potential, E_{redox}, may be tuned by choosing the constituents and temperature of the electrolysis.

Solar heating can decrease the energy to drive a range of electrolysis. Such processes can be described using data for the available entropy, S, enthalpy, H, and free-energy, G,[43] and they are identified by a negative isothermal temperature coefficient of the cell potential.[44] This coefficient $(dE/dT)_{isoth}$ is the derivative of the electromotive force of the isothermal cell:

$$(dE/dT)_{isoth} = \Delta S/nF = (\Delta H - \Delta G)/nFT \quad (1)$$

The starting process of modeling any STEP is the conventional expression of a generalized electrochemical process in a cell (specified as Electrode 1 | Electrolyte | Electrode 2) which drives an n-electron charge transfer electrolysis reaction, comprised of x reactants, R_i, with stoichiometric coefficients r_i, and yielding y products, C_i, with stoichiometric coefficients c_i.

Using the convention of $E = E_{cathode} - E_{anode}$ to describe the positive potential necessary to drive a nonspontaneous process by transfer of n electrons in the electrolysis reaction:

$$\sum\nolimits_{i=1 \text{ to } x} r_i R_i \rightarrow \sum\nolimits_{j=1 \text{ to } y} c_j C_j \quad (2)$$

At any electrolysis temperature, T_{STEP}, and at unit activity, the reaction has an electrochemical potential, E°_T. This may be calculated from thermochemical data, as:

$$E^\circ_T = -\Delta G^\circ(T = T_{STEP})/nF; E^\circ_{ambient} \equiv E^\circ_T(T_{ambient})$$

Here, $T_{ambient} = 298.15$ K $= 25\,^\circ$C, and:

$$\Delta G^\circ(T = T_{STEP}) = \sum\nolimits_j c_j(H^\circ(C_i,T) - TS^\circ(C_j,T)) - \sum\nolimits_i r_i(H^\circ(R_i,T) - TS^\circ(R_i,T)) \quad (3)$$

The temperature variation of the redox potentials and electrochemical mobilities can be large.[43–45] We use standard data, such as the National Institute of Standards and Technology (NIST) thermochemical data set to determine E°_T at unit activity. Activity coefficient variations can be substantial in aqueous media,[46–47] and they are incorporated by the Nernst expansion of Equation (3). The potential variation with activity (a = concentration × activity coefficient) for each reactant, R_i, and product, C_j, constituent of the electrolysis reaction is given by:

$$E_{T,a} = E^\circ_T - (RT/nF) \cdot \ln(\prod\nolimits_{i=1}(a_{R_i})r_i / \prod\nolimits_j (a_{C_j})c_j) \quad (4)$$

The thermoneutral potential, $E_{thermoneutral}$, is given by the enthalpy (ΔH, rather than ΔG) of a reaction necessary to sustain an electrochemical process without cooling; it tends to be nearly temperature independent and is given by:

$$E_{thermoneutral}\ (T_{STEP}) = -\Delta H(T)/nF; \quad \Delta H(T_{STEP}) = \sum\nolimits_i c_i H(C_i,T_{STEP}) - \sum\nolimits_j r_i H(R_j,T_{STEP}) \quad (5)$$

For example, the thermoneutral potential we calculate from the known thermochemical data for phenol oxidation to CO_2 at unit activities, from Equation (5), is (1.46 ± 0.01) V over the temperature range of 25–1400 °C.

In our study, two STEP modes (STEP and hybrid-STEP) are considered. Both STEP implementations can provide the thermoneutral energy to sustain a variety of electrolysis processes. As represented in the upper portion of Scheme 3, the standard electrolysis potential at room temperature, E°, can comprise a significant fraction of the thermoneutral potential. The STEP

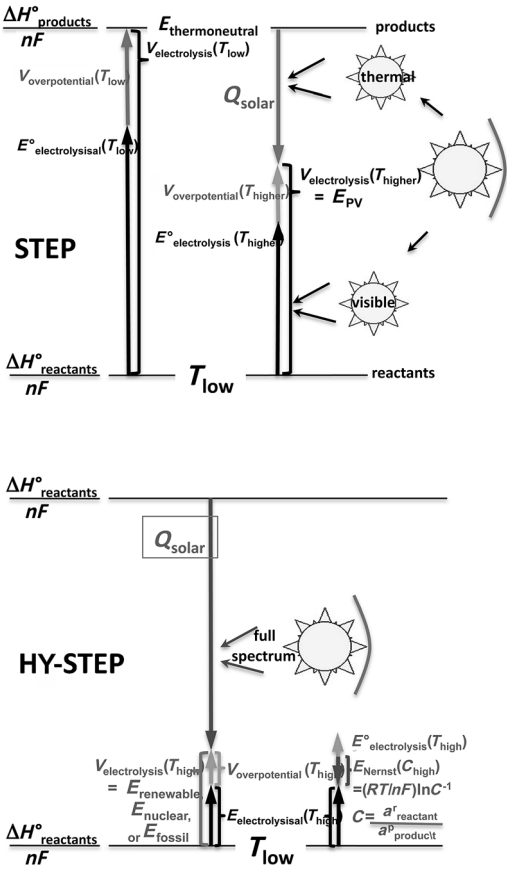

Scheme 3. Comparison of solar energy utilization in the STEP and hybrid-STEP processes implementations of the solar thermal electrochemical pollutant to carbon dioxide wastewater treatment.

mode, as compared to the room-temperature process, separates sunlight into thermal and visible radiation. The solar visible radiation generates electric charge which drives electrolysis charge transfer. The solar thermal component is shown heating the electrolysis reactants, which reduces both the E° at this higher temperature, and the overpotential. In the lower portion of the scheme, the hybrid-STEP mode does not separate sunlight into two parts, and instead directs all sunlight to heating the electrolysis reactants, thereby generating the highest T and smallest E, while the electrical energy for electrolysis is generated by a photovoltaic device run using a separate light source (or another renewable energy source). As shown on the right side, higher relative concentrations of the electrolysis reactant will further decrease the electrolysis potential.

STEP chemistry of wastewater treatment: Mechanistic pathways for the electrochemical oxidation of organic pollutants

The electrochemical oxidative removal of pollutants can occur either directly, through electron transfer between the anode and pollutant, or indirectly, through the generation of physical and electrochemical intermediates (for example, hydroxyl radicals). This latter process is usually called either "mediated oxidation" or "direct oxidation by radicals"[1] as described by Comninellis.[48] The complete oxidation of the organic substrate to carbon dioxide, or its partial, selective conversion into oxidation products is schematically represented in Scheme 4. When

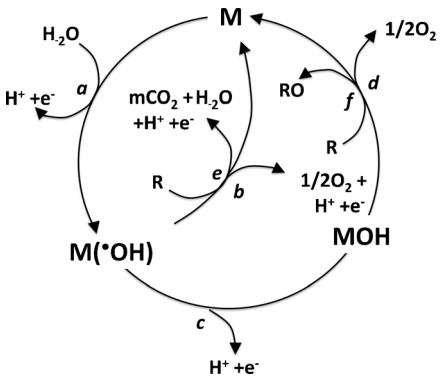

Scheme 4. Mechanistic scheme of the anodic oxidation of organic compounds on nonactive anodes (reactions a, b, and e) and on active anodes (reactions a, c, d and f). (From reference [56]).

a toxic, nondegradable organic is treated, the electrochemical conversion transforms the organic substrate into a variety of biocompatible organics or CO_2. The feasibility of this process depends on three parameters: (1) the generation of chemically or physically adsorbed hydroxyl radicals, (2) the nature of the anodic material and (3) the competition of this process with the oxygen evolution reaction. The electrochemical oxidation of some organics in aqueous media may take place without any loss in electrode activity except at high potentials.

As illustrated in Scheme 4, the pathway and individual mechanistic steps for the electrochemical oxidation of organics such as phenol, can be complex, with a variety of competing, potential intermediates. However, the combined oxidation of phenol to the final product, CO_2 is simply described, regardless of these intermediate processes. The principle anode, cathode, and full reactions occurring during the oxidization of phenol (C_6H_5OH) in aqueous solutions are summarized by Equations (6)–(8) as:

Anode, Electrochemical oxidation of phenol to carbon dioxide:

$$C_6H_5OH\ (l) + 11\,H_2O\ (l) \rightarrow 6\,CO_2(g) + 28\,H^+(l) + 28\,e^- \qquad (6)$$

Cathode, hydrogen evolution:

$$28\,H^+(l) + 28\,e^- \rightarrow 14\,H_2(g) \qquad (7)$$

Full cell reaction:

$$C_6H_5OH(l) + 11\,H_2O(l) \rightarrow 6\,CO_2(g) + 14\,H_2(g) \quad (8)$$

The aqueous phenol oxidation is described by Equation (8) with the calculated enthalpy from Equation (5) as $\Delta H^{\circ}(T_{25\,^{\circ}C}) = 947.6\ kJ\,mol^{-1}$, and the electrochemical potential from the free energy, Equation (5) of $E^{\circ}_{\text{phenol ox}}(25\,^{\circ}C) = 0.108$ V. In wastewater treatment, the electrolytic decomposition of the dominant species (water) leads to the simultaneous generation of further H_2, useful as a fuel:

$$H_2O(l) \rightarrow 1/2\,O_2(g) + H_2(g);\ E^{\circ}_{\text{water}}(25\,^{\circ}C) = 1.23\ V \quad (9)$$

The variation of the phenol electrolysis potential with temperature is calculated with Equation (5) and presented in Figure 1. The phenol oxidation potential decreases rapidly with

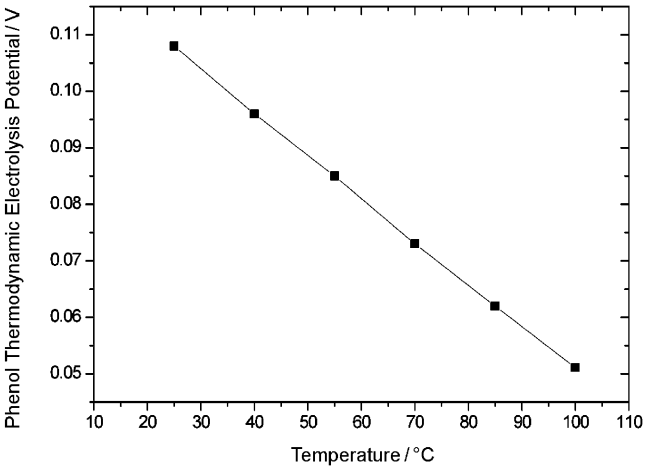

Figure 1. Theroretical, thermodynamic calculation of the electrochemical potential of phenol oxidation, Equation (8) at unit activities and with increasing temperature.

increasing temperature, which signifies that the STEP process may be readily applied to phenol electro-oxidation. For example, from 25 °C up to the H_2O boiling point of 100 °C, the phenol electrolysis potential in the aqueous phase decreases from 0.108 V to a low full cell oxidation electrolysis potential of only 0.051 V. This decrease provides a theoretical basis of the STEP process for effective and efficient solar removal of the organic pollutant from wastewater.

STEP solar to energy conversion efficiency of wastewater treatment

Both the STEP and hybrid-STEP configurations described in the theory section have been previously studied for the production of energetic molecules. In this study, only the experimentally simpler, hybrid-STEP mode is studied outdoors, as it eliminates the need for the beam splitter element. In this latter case, electricity generated by solar PV and heat supplied by a solar parabolic concentrator simultaneously drive the $E_{\text{electrolysis}}$ of water treatment. However, both modes are considered in this section to provide lower and upper bounds to the solar energy conversion efficiency.

In hybrid-STEP, the sunlight is not split and the full spectrum of sunlight heats the electrolysis cell, for which the electric charge is generated separately from renewable energy (as exemplified in this case by solar PV). Determination of the efficiency of hybrid-STEP with solar PV is straightforward in the domain in which the Coulombic efficiency is high, and in which the voltage required to drive the electrolysis, $V_{\text{electrolysis}}$, is less than the potential expressing the enthalpy needed to sustain the electrolyis, $E_{\text{thermoneutral}}$. Any higher voltage which would be applied, $V > E_{\text{thermoneutral}}$, would generate waste heat not needed to sustain the electrolysis. The electrolysis voltage includes the overpotential needed to drive the electrolysis potential described in Equation (4) at a current greater than zero ($V_{\text{electrolysis}} = E_{\text{Tra}} + V_{\text{overpotential}}$). Solar thermal energy is collected at an efficiency of $\eta_{\text{solar-thermal}}$ to decrease the energy for waste treatment from $E_{\text{thermoneutral}}$ to $V_{\text{electrolysis}}$, and then electrolysis is driven at a solar electric energy efficiency of $\eta_{\text{solar-electric}}$:

$$\eta_{\text{hybrid-STEPsolar}} = (\eta_{\text{solar-thermal}} \cdot (E_{\text{thermoneutral}} - V_{\text{electrolysis}}) + \eta_{\text{solar-electric}} \cdot V_{\text{electrolysis}})/E_{\text{thermoneutral}} \quad (10)$$

The black body absorption of sunlight with concentrating optics is straightforward, and experimentally efficient, typically ranging from 50 to 85%, which is greater than that of photovoltaic cell efficiencies, which typically have efficiencies ranging from ~6 to 40%. That is, in Equation (10), values of $\eta_{\text{solar-thermal}}$ are higher than $\eta_{\text{solar-electric}}$, and gains in efficiency occur in the limit as $V_{\text{electrolysis}}$ approaches 0. $V_{\text{electrolysis}} = 0$ is equivalent to the point at which thermochemical, rather than electrolytic wastewater treatment can occur. However, this generally occurs at high temperatures, which would require the additional vaporization energy to boil the wastewater, and often imposes material constraints. At lower temperature, small wastewater treatment values for $V_{\text{electrolysis}}$ can occur at higher reactant and lower product activities, as described in Equation (4).

The STEP solar energy conversion efficiency, η_{STEP}, is constrained by the coupling of the thermal, photovoltaic, and electrolysis conversion efficiencies, $\eta_{\text{solar-thermal}}$, $\eta_{\text{solar-electric}}$ and $\eta_{\text{electrolysis}}$. The electrolysis efficiency compares the stored (intrinsic) potential to the applied potential, $\eta_{\text{electrolysis}} = E^{\circ}_{\text{electrolysis}}(25\,^{\circ}C)/V_{\text{electrolysis}}(T)$.[10] $\eta_{\text{solar-thermal}}$ is coupled to the $\eta_{\text{electrolysis}}$, through $V_{\text{electrolysis}}(T)$ which decreases at higher temperature, T. The STEP solar conversion efficiency is the product of this relative gain in energy and the electronic solar efficiency:

$$\eta_{\text{STEP}} = \eta_{\text{solar-electric}} \cdot \eta_{\text{electrolysis}} = \eta_{\text{solar-electric}} \cdot E^{\circ}_{\text{electrolysis}}(25\,^{\circ}C)/V_{\text{electrolysis}}(T) \quad (11)$$

This latter conversion efficiency is an upper limit of the present experiment.

STEP experimental results of wastewater treatment

Pt cyclic voltammetry of phenol

Cyclic voltammetry (CV) of aqueous phenol was performed in 1000 ppm C_6H_5OH, swept at a rate of 50 mV sec^{-1} on anodic and cathodic platinum electrodes. The measured variation with temperature of the anodic peak potential (versus a SCE reference) and the anodic current density (at planar platinum electrodes) are summarized in Table 1.

Table 1. Summary of phenol cyclic voltammetry variation with temperature as measured on a platinum anode.

T [°C]	Anodic peak potential $V_{Oxidation\,peak}$ [V vs. SCE]	Anodic peak current $J_{Oxidation\,peak}$ [mA cm^{-2}]
20	0.95	1.30
40	0.88	1.50
60	0.76	2.40
80	0.50	2.80
90	0.45	3.20

In Table 1, it is seen that the anodic peak potential (of phenol oxidation) rapidly decreases with increasing solution temperature, while the anodic peak current density rapidly increases with increasing temperature. This trend correlates with the calculated decrease in thermodynamic potential presented in Figure 1. Due to this negative potential shift, the electrolysis energy required at high temperatures is less than at low temperature. The significant current increase implies that phenol oxidation kinetics are more facile at higher temperature, and demonstrates that a decrease in overpotential will be needed at higher electrolysis temperature.

High-surface-area electrocatalytic anode

In this study, La-doped PbO_2/Sn-Sb/Ti electrodes were utilized for their known activity towards phenol oxidation,[49] and they were specifically fabricated with high surface area to enhance this activity. Dimensionally stable anodes (DSAs) are characterized by a thin active coating (usually, a few microns) deposited on a base metal; Ti, Zr, Ta, Nb, and certain alloys of these metals have been effective compared to platinum for the electrochemical oxidation of phenol for wastewater treatment. La-doped PbO_2/Sn-Sb/Ti electrode is a DSA-type electrode. The Sn-Sb oxide interface layer is a coating which retains stability and, in conjunction with the base metal and the PbO_2 active layer, enables the electrocatalysis of phenol oxidation. The surface La-doping on the PbO_2 electrode exhibits superior performance compared to the corresponding nondoped electrodes.[50–55] Doped SnO_2 DSAs drive the electrochemical oxidation of phenol towards a full degradation to CO_2.[56]

The preparation of La-doped PbO_2/Sn-Sb/Ti consists of the following DSA electrode procedure:[3–4] first, coating a suitable solution of Sn-Sb salts ($SnCl_4$ and $SbCl_3$) on a polished and pretreated Ti foil (3 cm^2), then solvent evaporation at low temperature and thermal decomposition of metal salts into the oxide phase in 500 °C, electrocoating of the PbO_2 layer on the Sn-Sb/Ti layer; and finally electrodeposition of La-doping layer on the PbO_2/Sn-Sb/Ti in 1:0.25 (Pb:La, molarity ratio) doped amount at 50 °C for 2-hour electrodeposition time. Micromorphology and crystallography were measured by SEM (Hitachi S-4700) and XRD (Rigaku D/MAX-2200), respectively. A SEM image and XRD pattern of the La-doped PbO_2/Sn-Sb/Ti anode are shown in Figure 2 and 3.

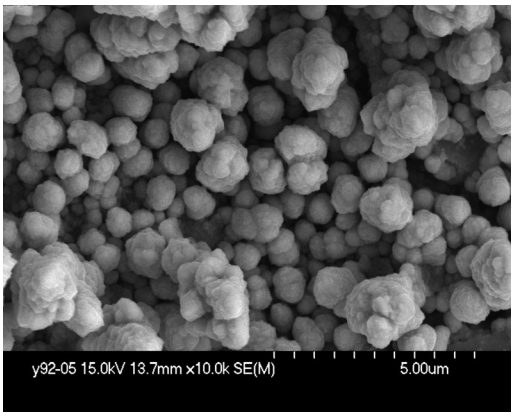

Figure 2. SEM image of optimized La-doped PbO_2/Sn-Sb/Ti anode.

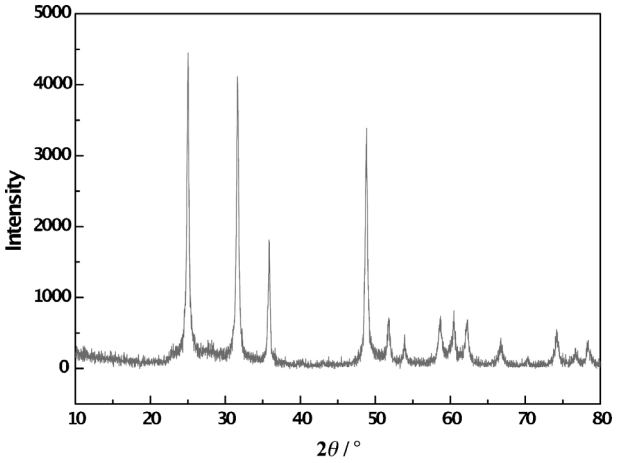

Figure 3. XRD pattern of optimized La-doped PbO_2/Sn-Sb/Ti anode.

STEP wastewater treatment prototypes

The wastewater treatment was experimentally characterized in the hybrid-STEP mode, incorporating a solar concentrator, a high temperature electrolyzer, and a PV module. As shown in Figure 4, the hybrid-STEP mode directs all concentrated solar energy to the electrolyzer.

In Figure 5, the STEP mode also utilizes a beam splitter which directs the super-band-gap (visible) sunlight to the PV module, and the sub-band-gap (thermal) sunlight to the electrolyzer. In principle, the latter mode is more efficient, recovering solar heat which could be used by the PV to heat the electrolyzer in order to make use of the complete solar spectrum. However, this latter configuration also requires an additional

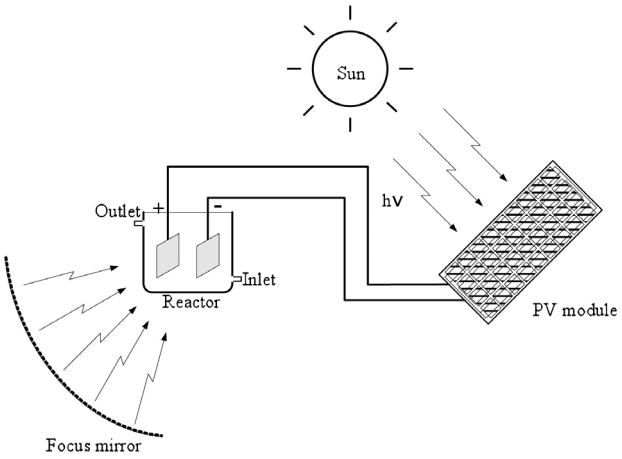

Figure 4. One system configuration of STEP wastewater experiments, the hybrid-STEP mode, in which the full solar spectrum is applied to electrolysis heating, and electrolysis charge is generated by a separate renewable solar, water, or wind electrical source, such as the PV illustrated.

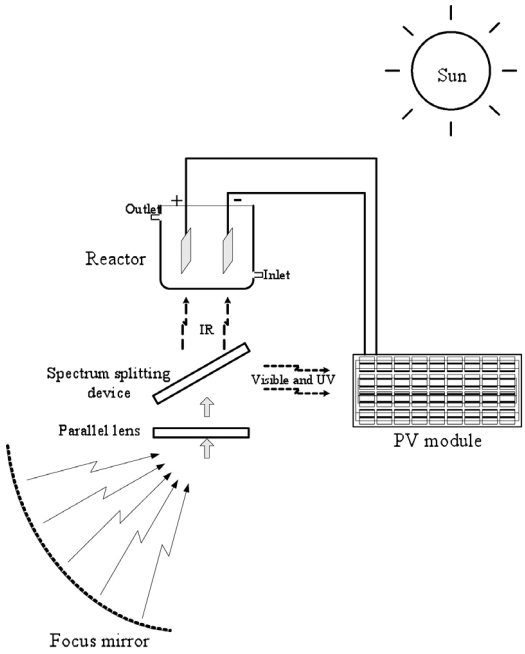

Figure 5. An alternative system configuration of STEP wastewater experiments (compared to the hybrid-STEP mode illustrated in Figure 4) in the beam splitting visible/infrared optical separation STEP mode.

optical component (a beam splitter, also termed a hot/cold mirror). The hybrid-STEP wastewater treatment operating system is presented in Figure 6.

The electrolyzer consists of a two-electrode electrochemical (glass) cell containing the optimized La-doped PbO_2/Sn-Sb/Ti anode, with a titanium sheet cathode. Water for treatment is pumped through the cell.

The reactor with the inlet and outlet tubes connected to a wastewater reservoir was centered at the focal point of a parabolic solar concentrator (diameter = 1.5 m), equipped to generate wastewater up to a 500 °C maximum temperature. The wastewater was pumped through the reservoir to the reactor

Figure 6. Experimental apparatus picture of the STEP wastewater experiments.

(temperature controlled by tuning the tracking control system). The polycrystalline silicon solar cells were used to generate 18 V at the maximum power point, with solar to electrical energy efficiencies of 18% under 1.5 sun illumination. The photovoltage applied to the electrolysis cell was controlled by a regulator. The retention time of wastewater in the cell was adjusted for the stationary state/flow state (returned to the reservoir for recycle) experiments.

Experimental removal of phenol by STEP wastewater treatment

Outdoor tests of phenolic wastewater treatment were conducted with the La-PbO_2/Sn-Sb/Ti anode (described above) and a titanium sheet cathode, making up a high temperature electrolysis cell powered by focusing sunlight in the hybrid-STEP mode. Specifically, concentrated sunlight decreases the observed phenol oxidation electrolysis voltage to 1 V.

Figure 7 presents the effectiveness of phenol oxidation by STEP wastewater treatment as a function of temperature and voltage. As shown in the figure, the STEP process occurs more effectively at high voltage, and high phenol conversion effi-

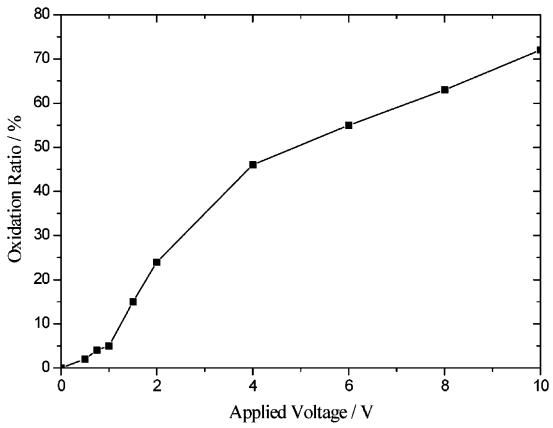

Figure 7. STEP oxidation ratio of phenol to applied voltage. The electrochemical cell consisted of a La-PbO_2/Sn-Sb/Ti anode and Ti-sheet cathode. The starting concentration of phenol was 100 ppm and the electrolysis was performed for 60 minutes at a temperature of 60 °C.

ciencies are evident. As seen, the phenol oxidation ratio is low at applied potentials below 1 V, and then with increased voltages the phenol oxidation efficiency increases. The minimum thermodynamic potential to split water is 1.23 V and this potential decreases with increasing temperature.[9] The critical electrolysis energy needed to oxidize phenol in an aqueous medium may be related to water splitting. The observed minimum potential to activate significant phenol oxidation appears to correlate with this minimum water splitting potential, and it may be mechanistically linked to a water splitting intermediate. We have previously observed that the overpotential and potential for water splitting decrease rapidly with increasing temperature.[42]

The solar concentrator readily brings the electrolyzer unit to the desired temperature. There is still additional capacity for light concentration from the parabolic reflector as well as photovoltage capacity from the PV in addition to what was utilized for this study. Hence, while oxidation ratios of phenol conversion and removal are quantitatively determined (system solar efficiencies will be provided in an expanded study), the system is presented as a STEP wastewater treatment proof of concept and principle. As evident in Figure 8, in the 1 V system, temperatures at or above 60 °C are conducive to a substantial electrochemical oxidative removal of phenol. The phenol oxidation efficiency increases from 2 to 36% by increasing the temperature with solar heating from 20 to 90 °C. A higher applied photovoltage of 10 V increased the oxidation efficiency compared to the 1 V-driven system, and as seen in the figure, the complete oxidative removal of the phenol is achieved at 90 °C.

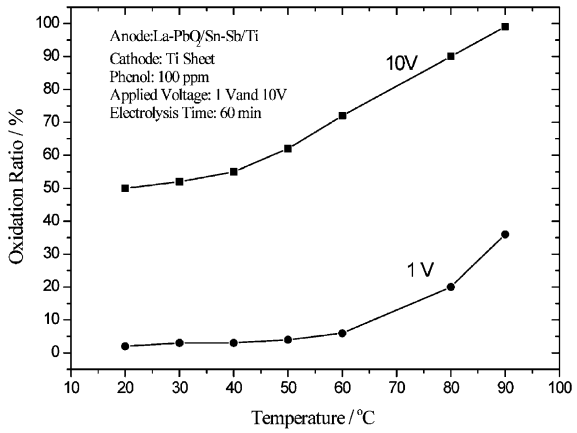

Figure 8. STEP oxidation ratio of phenol to temperature. The electrochemical cell consisted of a La-PbO_2/Sn-Sb/Ti anode and Ti-sheet cathode. The starting concentration of phenol was 100 ppm and the electrolysis was performed for 60 minutes at a voltage of either 1 V or 10 V.

UV/Vis analysis of the wastewater after extended (2 h) electrolysis, summarized in Figure 9, exhibits only the residual phenol, without evidence of a build-up of dissolved intermediate decomposition products, when the electrolysis is conducted at 90 °C (top), compared to incomplete oxidation and the build-up of intermediate oxidation products, when the electrolysis is conducted at 20 °C. Specifically, the top spectra exhibits the characteristic ~196, 210, and 270 nm peaks of aqueous phenol, and does not include the absorption peaks in the lower spectra at 245 and 255 nm evident of the co-existence of intermediate oxidation products.

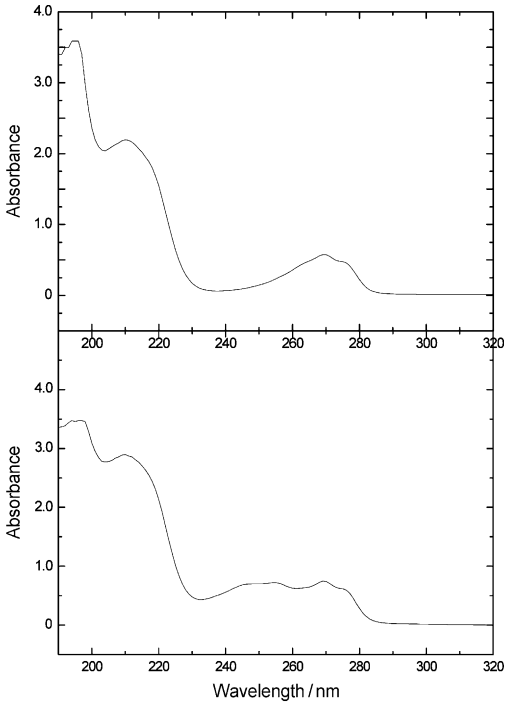

Figure 9. UV/Vis absorption spectroscopy of the wastewater solution after treatment at 90 °C (top) and 20 °C (bottom).

At 90 °C, the sole phenol carbon oxidation product is CO_2, as measured by GC in Figure 10 and UV/vis in Figure 9. Oxygen is also formed at the anode. Excess O_2 (as measured by GC and chemical oxygen demand (COD)) is accounted for by water splitting, and as seen in Figure 10, the ratio of the CO_2 to the H_2 product is significantly enhanced at 90 °C, which is consistent with the increasing efficiency of phenol oxidation at higher temperatures. At lower temperature, at both low and high applied potentials, the degradation of phenol is incomplete and it is accompanied by the formation of partial oxidation products. As previously discussed, this product mix can be complex, but presumably it includes intermediates consistent with Scheme 5.

The decrease in electrolysis potential with increasing temperature presents a low-free-energy opportunity for the STEP process. Solar thermal energy provides heat to decrease the phenol electrolysis potential. This provides a direct pathway for high solar-energy/phenol conversions and efficiencies. A novel and energy-free route for wastewater treatment is accomplished by the synergistic use of solar energy. The experiments present a substantial improvement in phenol oxidation ratio with increasing solar heating, and that the phenol electrolysis voltage decreases with increasing temperature.

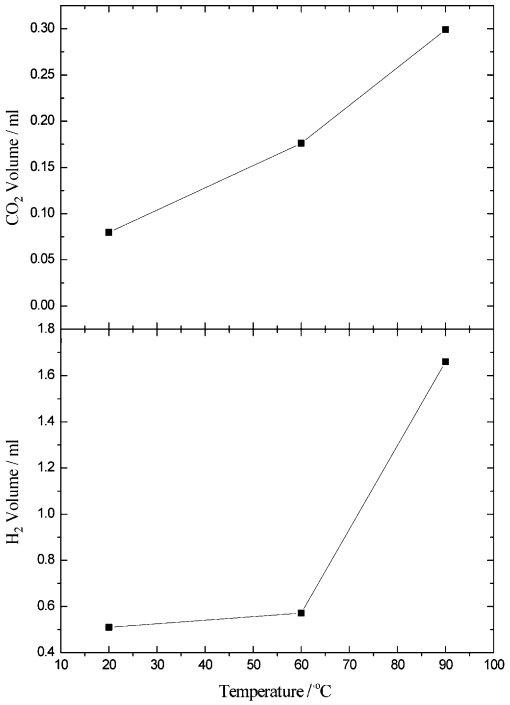

Figure 10. With increasing temperature, the amount of CO_2 anode product (top) and H_2 cathode product (bottom) increase, and the ratio of CO_2 to H_2 increases.

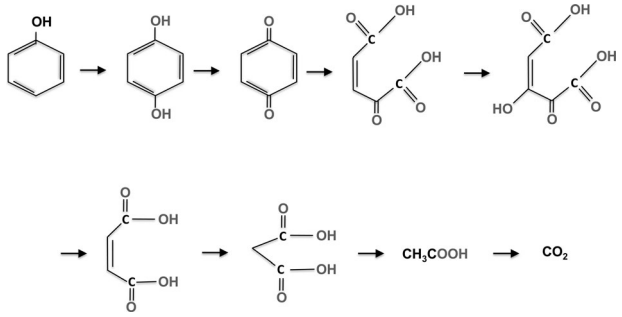

Scheme 5. Phenol oxidation pathways by hydroxyl radicals preceding the desired full oxidation to CO_2.

Conclusions

New water treatment processes that do not consume fossil fuels and are more environmentally benign towards the removal of organics are needed. In particular, new processes, driven by renewable energy, are needed to remove persistent (difficult to biodegrade) organics. An efficient solar-driven STEP approach to remove and convert pollutants in wastewater is introduced in this study. This new approach to organic oxidation combines solar thermal energy and electrolysis, to open a new, facile route to wastewater treatment. The STEP wastewater treatment system is characterized as a safe and sustainable process for efficient organic wastewater treatment and solar utilization.

Thermodynamic calculations are used to determine a specific low-energy pathway for organic wastewater treatment. The STEP solar-driven wastewater treatment was then experimentally investigated by treatment and removal of phenol. It is demonstrated that the thermodynamic and the kinetic energy barriers to drive wastewater treatment are decreased by the STEP process. This is respectively seen in a rapid decrease in the open circuit electrolysis potential, and in the electrolysis overpotential, for phenol electrolysis with increased solar heating.

Using the STEP process we demonstrated high temperature thermodynamic and kinetic advantages for the oxidative removal of phenol. These advantages cannot be accessed by photo-electrochemical systems. STEP pollutant oxidation overcomes the challenge faced by photo-electrocatalysis of sensitivity (degradation) of the photo-electrochemical surface at higher temperature. In photo-electrochemical systems, the semiconductor serves the twin functions of (i) a catalyst for electron exchange at the electrode/electrolyte interface and (ii) a photoabsorber. In semiconductors, photocorrosion increases with temperature and causes morphological changes to the surface, which can prevent effective photon absorption, electron/hole charge separation, or deactivate the catalyst.[57] Intricate photo-electrochemical electrode surfaces such as multilayered BiO_x-TiO_2, nanoporous TiO_2, or nanoparticles of Bi_2WO_6, while important room-temperature catalysts,[35–37] are increasingly susceptible to photocorrosion at higher temperature. The STEP process disassociates the roles of the photoabsorber and the electrocatalyst. A wide variety of electrocatalytic surfaces have been probed for phenol oxidation.[17–34] The high surface morphology electrocatalyst utilized here is stable at all temperatures investigated in the study, and conventional high performance PVs have a stability lifetime of years/decades. By using this electrocatalytic process we have demonstrated a new method for the electro-oxidation of organic contaminants.

The experimental ease of the STEP process for phenol removal in (simulated samples of) wastewater presents evidence that STEP pollutant oxidation will be applicable to a broad range of organic pollutants as will be investigated in an expanded study in the future.

Experimental Section

Chemicals and materials

Phenol (Aldrich, 99%), platinum foil (99.95% purity), titanium foil (pure, 99.9%) and chemical regents ($Pb(NO_3)_2$, $La(NO_3)_3$, $SnCl_4$ and $SbCl_3$) were used as received.

Electrolysis cell configuration

Cyclic voltammetry (CV) characterization experiments used a conventional three electrode configuration consisting of platinum foil working and counter electrodes separated by 1 cm, a saturated calomel electrode (SCE) reference electrode, and an aqueous phenol solution in a 50 mL beaker. STEP water treatment (phenol oxidation) experiments utilized a two-electrode system (the phenol active anode and cathode separated by the phenolic solution). Both Pt foils (3 cm^2) and non-noble electrodes (3 cm^2) were compared for the system. As described below, the non-noble electrode consisted of fabricated La-doped PbO_2/Sn-Sb/Ti anodes and titani-

um sheet cathodes. Potential voltage in all the measurements was applied by a potentiostat (BAS, Epsilon).

Analysis and oxidation ratio determination of phenol

Simulated contaminated water was prepared containing 100 ppm and 1000 ppm of phenol in 0.25 M Na_2SO_4, and this was used for making the wastewater samples. During the electrolysis process, samples were withdrawn at regular intervals. For each sample, the concentrations of phenol and its oxidation products were determined using UV/Vis spectroscopy (Shimadzu). The oxidation ratio of phenol was determined by dividing the concentration of remaining phenol by the concentration of original phenol and multiplying by 100%. The chemical oxygen demand (COD) was measured by the standard potassium dichromate titrimetric method. GC was conducted with a Shimadzu 2014 Multi Dimensional (2 columns) Gas Chromatograph.

Solar concentrator

An axially symmetrical, parabolic-cross-section reflector has the property of bringing parallel incident light to a point focus. Exposure to the sun concentrates sunlight and the focal area reaches high temperature. This is the basis for the use of this kind of solar thermal concentrator. In the experiments, a 1.5 m diameter, parabolic solar concentrator was used for high magnification and equipped with 2-dimensional tracking reflector control systems to maintain solar focus. The efficiency was tested for heating water as described by Equation (12):

$$\eta_{\text{solar-thermal}} = m \cdot c\ (t_e - t_i)/H \cdot A\ x\ 100\,\% \qquad (12)$$

in which, m is the water mass (kg), c is the water heat capacity ($kJ\,kg^{-1}\cdot{}^{\circ}C$), t_i is the initial temperature (°C), t_e is the final temperature (°C), H is the cumulative solar radiation ($kJ\,m^{-2}$), and A is the concentrator area (m^2). This parabolic solar concentrator was nominally measured with 65% efficiency for heating water. The solar concentrator consisted of 3 main parts. The parabolic reflector concentrates sunlight from a 1.5 m diameter to as little as 0.05 m, but it may be defocused to attain lower levels of solar concentration. The control system allows the reflector to be set facing the sun and holds the reactor at the focal point regardless of the reflector tilt angle. The stand holds the other two components together and allows the reactor to be rotated to follow the sun as it moves across the sky. Wastewater (or steam) is produced by passing a flow reactor (or reservoir) at the focus point of the solar concentrator at temperatures ranging from room temperature to a maximum of 500 °C, tuned by the tracking/defocussing control system. The solar concentrator unit provided excess heat and was defocused to achieve lower temperatures.

Solar electronic

Polycrystalline silicon solar module cells (3 W/12 V, VUAVA, China) were used to provide electric charge for the electrolysis. The module is 15.5 cm × 22.5 cm with multiple (36) series connected cells. The module was characterized in standard irradiance of AM1.5 ($1000\,W\,m^{-2}$) and used a temperature of 25 °C. Under illumination the cells yielded an open circuit voltage (V_{oc}) of 21.8 V, a short circuit current (I_{sc}): 0.2 A, a maximum power voltage (V_{mp}) of 18 V, a maximum power current (I_{mp}) of 0.17 A, a maximum power (P_{max}) of 3 W, and a solar efficiency of 18%.

Acknowledgements

The authors (B.W. and H.W.) are grateful to the National Natural Science Foundation of China for support, 51146008.

Keywords: electrochemistry · oxidation · photochemistry · solar energy · wastewater treatment

[1] C. A. Martinez-Huitle, S. Ferro, *Chem. Soc. Rev.* **2006**, *35*, 1324 – 1340.
[2] O. Scialdone, *Electrochim. Acta* **2009**, *54*, 6140 – 6147.
[3] K. Rajeshwar, J. G. Ibanez, G. M. Swain, *J. Appl. Electrochem.* **1994**, *24*, 1077 – 1091.
[4] O. Simond, Ch. Comninellis, *Electrochim. Acta* **1997**, *42*, 2013.
[5] G. Chen, *Sep. Purif. Technol.* **2004**, *38*, 11.
[6] O. Scialdone, A. Galia, G. Filardo, *Electrochim. Acta* **2008**, *53*, 7220.
[7] S. Licht, X. Yu, *Environ. Sci. Technol.* **2005**, *39*, 8071.
[8] *On Solar Hydrogen & Nanotechnology* (Ed: L. Vayssieres), Wiley-VCH, Weinheim, Germany, **2009**.
[9] S. Licht, *J. Phys. Chem. C* **2009**, *113*, 16283.
[10] S. Licht, B. Wang, H. Wu, *J. Phys. Chem. C* **2011**, *115*, 11803.
[11] S. Licht, B. Wang, S. Ghosh, H. Ayub, D. Jiang, J. Ganely, *J. Phys. Chem. Lett.* **2010**, *1*, 2363.
[12] S. Licht, B. Wang, *Chem. Commun.* **2010**, *46*, 7004; S. Licht, H. Wu, Z. Zhang, H. Zyub, *Chem. Commun.* **2011**, *47*, 3081.
[13] S. Licht, H. Wu, *J. Phys. Chem. C* **2011**, *115*, 25138.
[14] S. Licht, *Adv. Mater.* **2011**, *23*, 5592.
[15] S. Licht, O. Chitayat, H. Bergmann, A. Dick, H. Ayub, S. Ghosh, *Int. J. Hydrogen Energy* **2010**, *35*, 10867.
[16] S. Licht, H. Wu, C. Hettige, B. Wang, J. Asercion, J. Lau, J. Stuart, *Chem. Commun.* **2012**, *48*, 6019.
[17] Y. S. Bashtan, V. A. Bagrii, *J. Water Chem. Technol.* **2012**, *34*, 24.
[18] D. Lu, Y. Zhang, S. Niu, L. Wang, S. Lin, C. Wang, W. Ye, C. Yan, *Biodegradation* **2012**, *23*, 209.
[19] J. Sun, H. Lu, H. Lin, L. Su, W. Huang, H. Li, T. Cui, *Sep. Purif. Technol.* **2012**, *88*, 116.
[20] M. Tian, S. S. Thind, M. Simko, F. Gao, A. Chen, *J. Phys. Chem. A* **2012**, *116*, 2927.
[21] C. di Luca, F. Ivorra, P. Massa, R. Fenoglio, *Ind. Eng. Chem. Res.* **2012**, *51*, 8979 – 8984.
[22] E. Bazrafshan, H. Biglari, M. Amir Hossein, *Fresenius Environ. Bull.* **2012**, *21*, 364.
[23] M. A. M. Cartaxo, K. Ablad, J. Douch, Y. Berghoute, M. Hamdani, M. H. Mendonça, J. M. F. Nogueira, M. I. S. Pereira, *Chemosphere* **2012**, *86*, 341.
[24] X. Zhu, J. Ni, J. Wei, P. Chen, *Electrochim. Acta* **2011**, *56*, 9439.
[25] J. Wei, X. Zhu, J. Ni, *Electrochim. Acta* **2011**, *56*, 5310.
[26] I. D. Santos, S. B. Gabriel, J. C. Afonso, A. J. Bourdot Dutra, *Mater. Res.* **2011**, *14*, 408.
[27] T. A. Enache, A. M. Oliveira-Brett, *J. Electroanal. Chem.* **2011**, *655*, 9.
[28] I. D. Santos, J. C. Afonso, A. J. Bourdot Dutra, *J. Braz. Chem. Soc.* **2011**, *22*, 875.
[29] H. J. Wang, X. J. Wu, Y. L. Wang, Z. B. Jiao, S. W. Yan, L. H. Huang, *Chin. J. Catal.* **2011**, *32*, 637.
[30] J. L. N. Xavier, E. Ortega, J. Z. Ferreira, A. M. Bernardes, V. Pérez-Herranz, *Int. J. Electrochem. Sci.* **2011**, *6*, 622.
[31] G. V. Kornienko, N. V. Chaenko, N. G. Maksimov, A. M. Kosheleva, V. L. Kornienko, *Russ. J. Electrochem.* **2011**, *47*, 225.
[32] Y. H. Cui, Y. J. Feng, X. Y. Li, *Chem. Eng. Technol.* **2011**, *34*, 265.
[33] Y. Zhao, Y. Ding, L. Wang, X. Wang, *Water Sci. Technol.* **2011**, *63*, 1950.
[34] X. Zhu, J. Ni, J. Wei, X. Xing, H. Li, Y. Jiang, *J. Hazard. Mater.* **2010**, *184*, 493.
[35] H. Park, A. Bak, Y. Y. Ahn, J. Choi, M. R. Hoffmannn, *J. Hazard. Mater.* **2012**, *211*, 47.
[36] D. Manllor-Satoca, T. Lana-Villarreal, R. Gómez, *Langmuir* **2011**, *27*, 15312.
[37] S. Sun, W. Wang, J. Xu, L. Wang, Z. Zhang, *Appl. Catal. B* **2011**, *106*, 559.
[38] C. Costentin, C. Louault, M. Robert, J.-M. Savéant, *Proc. Natl. Acad. Sci. USA* **2009**, *106*, 18143.
[39] Z. Zou, Y. Ye, K. Sayama, H. Arakawa, *Nature* **2001**, *414*, 625.

[40] S. Licht, B. Wang, S. Mukerji, T. Soga, M. Umento, H. Tributsh, *J. Phys. Chem. B* **2000**, *104*, 8920.
[41] S. Licht, *J. Phys. Chem. B* **2001**, *105*, 6281.
[42] S. Licht, L. Halperin, M. Kalina, M. Zidman, N. Halperin, *Chem. Commun.* **2003**, 3006.
[43] M. W. Chase, *J. Phys. Chem. Ref. Data* **1998**, *9*, 1. Data available from: http://webbook.nist.gov/chemistry/form-ser.html (accessed September 2012).
[44] A. J. deBethune, T. S. Licht, *J. Electrochem. Soc.* **1959**, *106*, 616.
[45] T. S. Light, S. Licht, A. C. Bevilacqua, *Electrochem. Solid-State Lett.* **2005**, *8*, E16.
[46] S. Licht, *Anal. Chem.* **1985**, *57*, 514.
[47] S. Licht, K. Longo, D. Peramunage, F. Forouzan, *J. Electroanal. Chem.* **1991**, *318*, 119.
[48] Ch. Comninellis, *Electrochim. Acta* **1994**, *39*, 1857 – 1862.
[49] S. Trasatti, *Electrochim. Acta* **2000**, *45*, 2377 – 2385.
[50] X. Yang, R. Zou, F. Huo, D. Cai, D. Xiao, *J. Hazard. Mater.* **2009**, *164*, 367 – 373.
[51] J. Kong, S. Shi, X. Zhu, J. Ni, *J. Environ. Sci.* **2007**, *19*, 1380 – 1386.
[52] S. Abaci, U. Tamer, K. Pekmez, *Appl. Surf. Sci.* **2005**, *240*, 112 – 119.
[53] A. M. Polcaro, S. Palmas, F. Renoldi, M. Mascia, *Electrochim. Acta* **2000**, *46*, 389 – 394.
[54] Y. J. Feng, X. Y. Li, *Water Res.* **2003**, *37*, 2399 – 2407.
[55] S. Song, L. Zhan, Z. He, L. Lin, J. Tu, Z. Zhang, J. Chen, L. Xu, *J. Hazard. Mater.* **2010**, *175*, 614 – 621.
[56] Ch. Comninellis, C. Pulgarin, *J. Appl. Electrochem.* **1993**, *23*, 108 – 112.
[57] *Semiconductor Electrodes and Photoelectrochemistry* (Ed.: S. Licht), Wiley-VCH, Weinheim, Germany, **2002**.

Received: May 3, 2012
Revised: June 4, 2012
Published online on ■■ ■■, 0000

B. Wang, H. Wu, G. Zhang, S. Licht**

■■ – ■■

STEP Wastewater Treatment: A Solar Thermal Electrochemical Process for Pollutant Oxidation

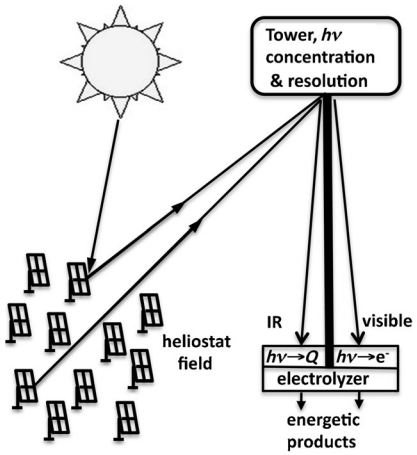

Single STEP: A sustainable methodology of wastewater treatment is presented based on the generalized solar thermal electrochemical production (STEP) process for the conversion and use of solar energy. The STEP process utilizes long-wavelength solar radiation to heat the electrochemical cell, thereby improving both the thermodynamics and kinetics for photovoltaic-driven oxidation. As a proof of concept, the STEP process was utilized to oxidize and remove phenol as a contaminant from artificial wastewater.

